Full Paper

Propellants, Explosives, Pyrotechnics

DOI: 10.1002/prep.201800004

Fabrication of Ultra-Fine TATB/HMX Cocrystal Using a Compound Solvent

Conghua Hou,*[a] Yuanping Zhang,*[a] Yunge Chen,[a] Xinlei Jia,[a] Shimin Zhang,[a] and Yingxin Tan[a]

Abstract: A novel energetic cocrystal predicted to exhibit greater power and lower sensitivity, consisting of 1,3,5-triamino-2,4,6-trinitrobenzene (TATB) and cyclotetramethylenetetranitramine (HMX) is presented. The TATB/HMX cocrystals were prepared using a compound solvent of [Emim]Ac and DMSO at 80 °C by recrystallization. Structural characterizations and thermal properties of the raw materials and cocrystals were systematically investigated by scanning electron microscopy (SEM), X-ray diffraction, fourier-transform infrared spectroscopy, fourier transform raman spectroscopy and differential scanning calorimetry. The SEM results indicated that microparticles are hexagonal in shape and ~2 μm in size. The formation of cocrystals originates from the N–H···O hydrogen bonding between -NO_2 (HMX) and -NH_2 (TATB). Naturally, compared to raw HMX, the impact sensitivity of the cocrystals is reduced. The EXPLO5 program showed TATB/HMX with desirable detonation performance.

Keywords: TATB/HMX cocrystal · [Emim]Ac/DMSO compound solvent · ultra-fine · performance

1 Introduction

With the development of modern warfare, more stringent demands are placed on weapon systems. In the pursuit of high energy density, safety and performance play equally important roles. As a consequence, high-energy insensitive explosives have been proposed and prepared to resolve the contradiction without affecting the power of highly explosive ammunition [1–4]. Accordingly, considerable effort has been committed to the exploration of an explosive with higher explosive performance and lower sensitivity. At present, the performance and sensitivity of explosives can be tuned by three traditional methods, including synthesizing new explosives, controlling crystal morphology, and manufacturing plastic bonded explosives. However, these traditional modification methods have not changed the explosives crystal structure and internal composition. Therefore, cocrystallization [5–7] as a new technique was proposed for the preparation of energetic materials. Cocrystallization is a technology to improve the performance of existing energetic materials by modifying intermolecular forces without altering the original molecular structure of explosives.

Cyclotetramethylenetetranitramine (HMX) is a molecular explosive outstanding in detonation performance, but its widespread implementation has been hindered due to its high mechanical sensitivity [8]. In the recent past the technology of explosive cocrystals has been investigated. A CL-20/HMX cocrystal explosive in a 2:1 molar ratio was prepared by Bolton et al. [9]. Nano-CL-20/HMX cocrystal explosive was prepared by the spray drying method by An et al. [10]. Lin et al. [11–15] designed and synthesized the cocrystal of HMX/N-methyl-2-pyrrolidone, HMX/1,3-dimethyl-2-imidazoli-dinone, HMX/pyridine-N-oxide by the solution evaporation method and revealed the assembly rules of HMX-cocrystal based on the crystal structure analysis and DFT calculation. HMX/NTO and HMX/LLM-105 cocrystals were synthesized and studied as well. Li et al. [16] prepared nano HMX/TNT cocrystals with size ranging from 50 nm to 200 nm by the spray drying method.

1,3,5-triamino-2,4,6-trinitrobenzene (TATB) [17] is well known to be very insensitive to heat, friction, and impact, and has good thermal stability and impact sensitivity. In this paper we present cocrystal explosives composed of HMX and TATB, which can meet the requirements of high energy and insensitivity. The HMX/TATB cocrystal was designed based on crystal engineering, and its crystal structure was predicted by the polymorph predictor method in a molecular dynamics simulation by Wei and coworkers [18].

In this study, TATB and HMX were first dissolved in a mixture of [Emim]Ac and DMSO in a molar ratio of 5:95 as the co-solvent. Meanwhile, Molecular dynamics (MD) method of Materials Studio software and Quantum Chemica was explored for the feasibility of cocrystal formation. TATB/HMX cocrystal explosive was obtained at 80 °C in [Emim]Ac/DMSO composite solvent. Furthermore, structural characterizations and thermal properties of the raw materials and cocrystals were systematically investigated in detail.

[a] *C. Hou, Y. Zhang, Y. Chen, X. Jia, S. Zhang, Y. Tan*
School of Environment and Safety Engineering, North University of China, Taiyuan 030051, China

2 Experimental

2.1 Materials and Sample Preparation

HMX and TATB were supplied by Gansu Yinguang Chemical Industry Group Co. Ltd. DMSO and [Emim]Ac were provided by Tianjin Chemical Reagent Factory and Shanghai Chengjie Chemical Co., Ltd., respectively.

TATB/HMX cocrystals were prepared by recrystallization. The preparation process is as follows: first, 1 g TATB and 2.677 g HMX (molar ratio of 3:7) were added to 200 mL composite solvent [Emim]Ac/DMSO in a molar ratio of 5:95. Then, the system was stirred for 3 h at 80 °C under high-intensity ultrasonic irradiation with an output acoustic power of 240 W at a frequency of 40 kHz until the raw materials dissolved completely to form a co-solution. In the next step, 2000 mL ultrapure water as the non-solvent was slowly added to the system under stirring at a speed of 500 rpm. The resulting precipitate was vacuum filtered, washed five times, and freeze dried for 5 h, affording TATB/HMX cocrystals.

2.2 Molecular Dynamics (MD) Simulation

Molecular dynamics (MD) simulations with the COMPASS force field of Materials Studio software (MS) were used to establish 4 * 2 * 3 β-HMX cells, TATB cells, TATB/HMX cocrystal (molar ratio of 1:1) cells by the Andersen temperature control method with a temperature of 298 K and a step length of 1 fs. The morphology module was used to predict the cocrystal growth planes of HMX and TATB.

2.3 Characterization

Field-emission scanning electron microscopy (FESEM, S4700 Hitachi, Ltd.Japan) was used to visualize the changes in morphology, size, and micro-structure of the samples. The as-obtained TATB/HMX cocrystals were dispersed on conductive carbon adhesive tape to attach to an FESEM stub and then gold-coated for SEM investigation.

The crystal form of TATB/HMX cocrystal was determined by X-ray powder diffraction (XRD), Dandong Haoyuan Corporation, Liaoning, China. XRD patterns were recorded using a Bruker D8 Advance diffractometer at a voltage of 40 kV and a current of 30 mA using Cu–Kα radiation at $\lambda =$ 1.5418 Å.

Infrared spectra were measured using a Nicolet 380 Fourier transform infrared (FTIR) spectrometer (KBr pellets, Thermo Fisher Scientific, Waltham, MA, USA). FTIR transmission spectra were generated using an FTIR spectrophotometer (Nicolet 6700, Thermo Scientific).

Fourier Transform Raman spectroscopy (FT-Raman, Bio Rad Co., Ltd. USA) was used to explore the formation of cocrystals. The Raman excitation light with a power of 0.5 mW was provided by 532 nm line of an argon ion laser. For each sample, the spectrum was obtained by averaging 20 scans with a measurement time of 5 s per scan.

The thermal properties were characterized by DSC-131 (SETARAM, France). The DSC conditions used are as follows: sample mass: 0.7 mg; heating rate: 5, 10, and 20 K/min; nitrogen atmosphere (flow rate: 20 mL/min).

2.4 Sensitivity Test

The impact sensitivity test was performed using a home-built Type 12 drop hammer apparatus according to GJB-772A-97 standard method 601.2. The samples (35 ± 1 mg) were subjected to an impact of a 2.500 ± 0.002 kg hammer and H_{50}, representing the drop height of 50% explosion probability [19, 20].

3 Results and Discussion

3.1 Computational Predictions

The COMPASS force field was used to calculate the five main growth planes of the β-HMX crystal in the attachment energy (AE) model of the Morphology module. The adhesion energy, the van Edward force, and the electrostatic force of the crystal face are shown in Table 1, indicating that the attachment energy of the (0 1 1) surface of the β-HMX is the smallest and can be considered as the main growth surface to form cocrystal with the TATB molecule on this surface. The equilibrium structure of TATB/HMX cocrystal was obtained by simulation as shown in Figure 1. The simulation results show that hydrogen bonds can be formed between TATB and HMX molecules including three N–H···O hydrogen bonds.

Table 1. The main growth plane of the crystal of beta-HMX.

crystal surface	Eatt(Total)/ (kJl/mol)	Eatt(vdW)/ (kJ/mol)	Eatt(Electrostantic)/ (kJ/mol)
(0 1 1)	−115.39	−82.19	−33.20
(0 2 0)	−165.04	−89.43	−75.74
(1 1-1)	−172.83	−88.47	−84.36
(1 0 0)	−223.11	−114.00	−109.11
(1 0-2)	−190.75	−100.73	−90.01

3.2 SEM

The morphology and structure of raw TATB, HMX, and TATB/HMX cocrystals were probed by SEM. The results are shown in the Figure 2. As shown in Figure 2(a), the TATB particles exhibited a layered structure with particle size of 10 μm.

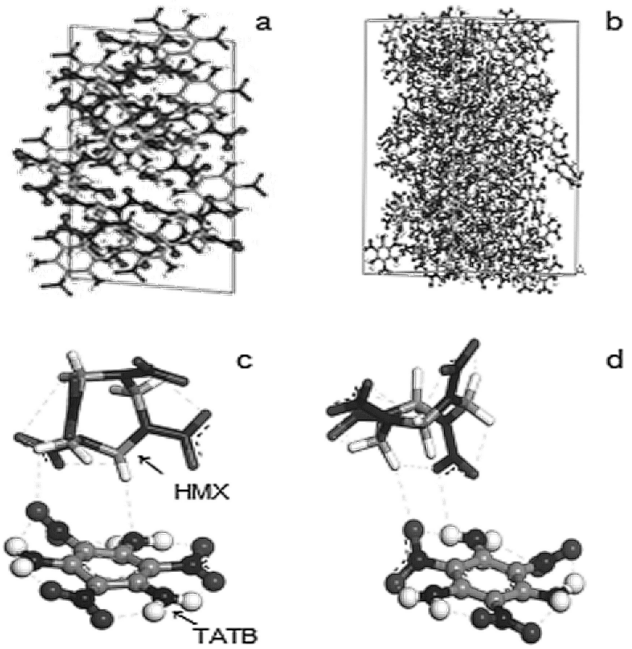

Figure 1. Structure of HMX/TATB molecule. The dotted line shows the hydrogen bonds.

The HMX particles in Figure 2(b) act as slender rod like crystals with an average size of 15 μm. Figure 2(c) clearly shows that the ultra-fine TATB/HMX cocrystals had hexagonal morphology, unlike that of TATB and HMX. The particle size of majority of the cocrystals is ~2 μm, which is less than that of the raw material.

3.3 XRD

The crystalline phases and composition of samples were identified by XRD. Figure 3 shows the XRD patterns of TATB, HMX, and cocrystal particles. There is a significant displacement of the diffraction peaks of TATB/HMX cocrystals compared to those of TATB and HMX. The peaks of diffraction of raw HMX at 20.45°, 23.00°, and 31.91° did not appear in the patterns of TATB/HMX cocrystal. The peaks of diffraction of

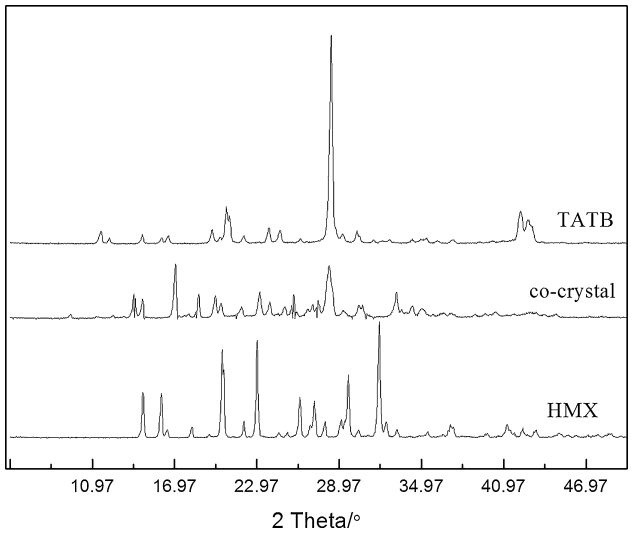

Figure 3. XRD pattern of TATB, HMX, and TATB/HMX cocrystals.

raw TATB at 20.87°, 42.14°, and 42.80° also did not appear. In addition, new diffraction peaks at 16.97° and 33.47° of cocrystal appeared. The results suggested that the samples are not simply mixed, but HMX and TATB interacted to form a new cocrystal. This interaction is probably caused by the intermolecular hydrogen bond, van der Waals force, and a π bond collectively or on their own.

3.4 FTIR

The FTIR spectra of raw TATB, HMX, and TATB/HMX are shown in Figure 4. The assignments of the major bands of samples are listed in Table 2. Compared to the characteristic peaks of TATB and HMX, new band of TATB/HMX cocrystal was observed at 1020 cm^{-1}. The characteristic bands of TATB at 3470 and 1610 cm^{-1} corresponding to the vibration of $-NH_2$ and $C-NH_2$, and shifted to 3440, and 1570 cm^{-1}, respectively. Similarly, the peaks of HMX at 1560 and 1350 cm^{-1} corresponding to the vibration of aliphatic $-NO_2$ and $-CH_2$, respectively, shifted to 1570 and 1320 cm^{-1}. These changes can be attributed to the formation of the hy-

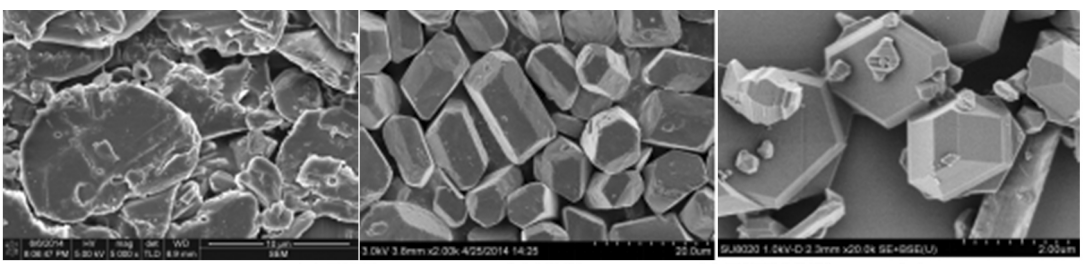

Figure 2. SEM images of TATB, HMX, and TATB/HMX cocrystal.

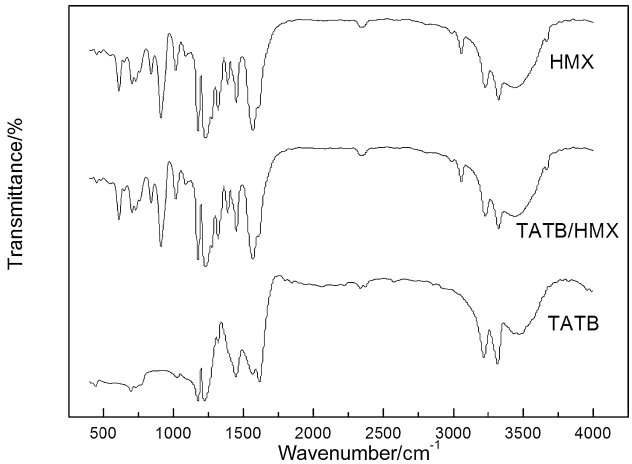

Figure 4. FTIR spectra of TATB, HMX, and TATB/HMX cocrystals.

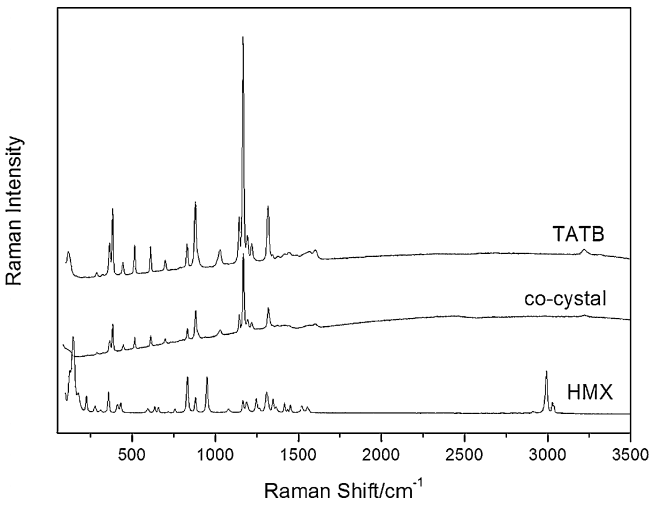

Figure 5. FT-Raman spectra of TATB, HMX, and TATB/HMX cocrystals (cm^{-1}).

drogen bonding between $-NO_2$ (HMX) and $-NH_2$ (TATB). Moreover, the N–O···H shortened the distance between HMX molecules and TATB molecules in the cocrystal structure.

3.5 FT-Raman

Raman spectroscopy is a very useful tool to characterize cocrystals [21,22]. The FT-Raman spectra of HMX, TATB, and HMX/TATB cocrystal are presented in Figure 5. The assignments of the major bands of samples are listed in Table 3, indicating that the absorption peaks of TATB at 3224.2, 1604.2, 1317.7, and 1167.2 cm^{-1} corresponding to the NH_2, C–NO_2, NO_2, and C-NH_2, respectively, have offset in the cocrystals. The characteristic vibration peaks at 1556.4, 1347.5, 145, and 879.2 cm^{-1} separately in the HMX infrared spectrum are related to the $-NO_2$ and C–N–C of the ring of HMX. All these changes imply a significant change in the cocrystal structure owing to the intermolecular interactions between HMX and TATB molecules and are consistent with the infrared spectrum and hydrogen bonds simulated by MD. At the same time, those shifts confirm the formation of cocrystal, as supported by the X-ray characterization.

3.6 DSC

The thermal properties of the TATB, HMX and TATB/HMX cocrystal were studied by DSC. The experimental data are listed in Table 4. As shown in Figure 6 and Table 4, the initial decomposition temperature and peak temperature of TATB/HMX cocrystals gradually shifted toward a higher temperature compared to that of HMX. The second peaks discovered in the curve of cocrystals significantly weakened and shifted to the left. The lower the heating rate, the more weakened the peaks became and can be ascribed to the interaction between HMX and TATB. The results reveal that the thermal decomposition properties of the cocrystal did not change significantly, indicating that the formation of in-

Table 2. FTIR spectra of TATB, HMX, and TATB/HMX cocrystal (cm^{-1}).

Assignment	TATB	TATB/HMX cocrystal	HMX	Assignment
$-NH_2$ out-of-plane deformation	696	611	600	Ring deformation + NO_2 out-of-plane deformation
	–	910	947	Ring deformation
	–	1020	–	
Ring in-plane deformation	1180	1180	1200	–N–N stretching + $-NO_2$ symmetric stretching
$-NO_2$ symmetric stretching	1230	1230	1290	N–N stretching + NO_2 symmetric stretching
	–	1320	1350	$-CH_2$ deformation
Ring in-plane deformation	1450	1450	1460	
–C–N stretching(C-NH_2)	1610	1570	1560	$-NO_2$ asymmetric stretching
	–	3050	3050	$-CH_2$ stretching
$-NH_2$ stretching	3220	3220	–	
$-NH_2$ stretching	3320	3320	–	
$-NH_2$ stretching	3470	3440	3400	

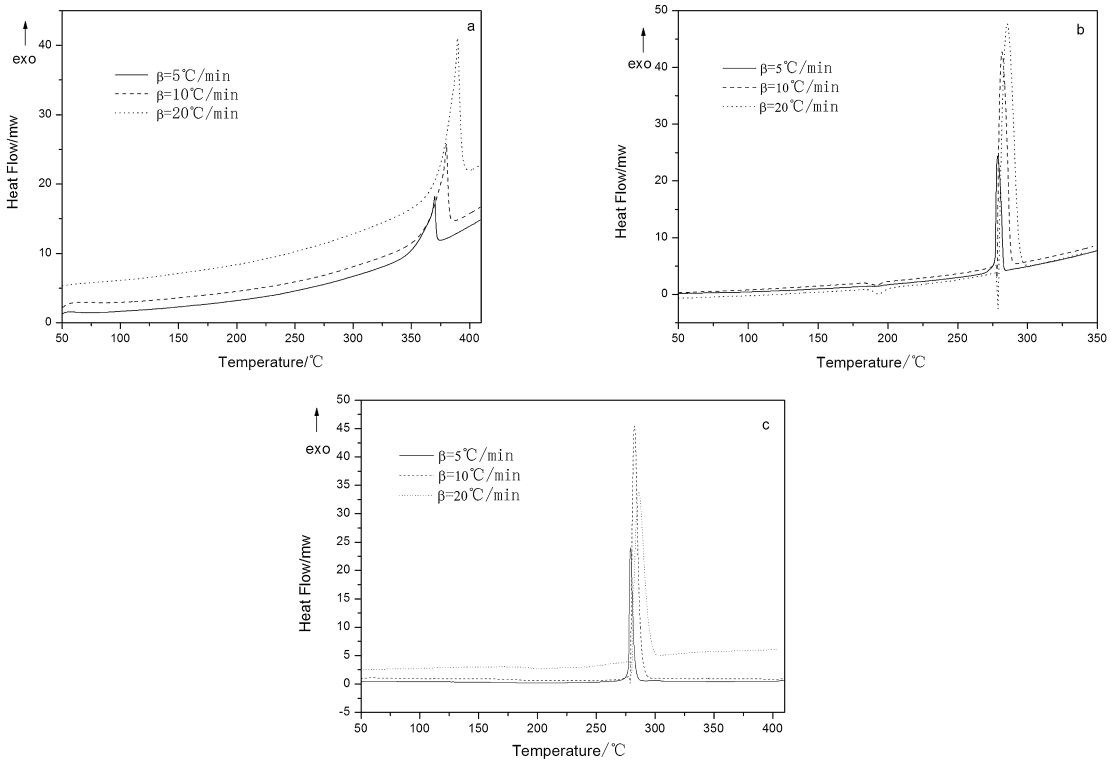

Figure 6. DSC curves of TATB, HMX, and TATB/HMX cocrystals.

Table 3. Raman absorption peaks of TATB, HMX, and TATB/HMX cocrystal (cm^{-1})

Assignments	TATB	TATB/HMX cocrystal	HMX	Assignments
-NH_2 stretching vibration	3224.2	3222.8	–	
–C–N stretching vibration(C–NO_2)	1604.2	1605.6	–	
	-	1567.3	1556.4	–NO_2 asymmetric symmetric stretching
–NO_2 stretching vibration	1317.7	1318.9	1347.5	N–N stretch vibration
–C–N stretching(C–NH_2)	1167.2	1168.3	–	
ring stretching vibration	1022.8	1028.6	–	
	–	881.7	879.2	ring stretching
ring deformation	384.2	383	–	
	–	366.8	359.1	ring deformation
			145	NO_2 deformation

Table 4. DSC test results of TATB, HMX, and TATB/HMX cocrystals.

samples	β/(°C/min)	T_0	T_p
TATB	5	364.79	370.14
	10	374.91	380.21
	20	383.43	389.82
HMX	5	276.67	278.78
	10	278.28	281.83
	20	279.08	285.47
TATB/HMX	5	280.78	281.09
	10	280.38	283.25
	20	280.78	286.93

ter-molecular forces was slightly sufficient to affect the exothermic decomposition. To further confirm how the thermal properties really affected, more reliable experiments were carried out later.

3.7 Impact Sensitivity

To investigate the safety performance of the cocrystals, impact sensitivity test was performed. The cocrystals exhibited an H_{50} of 100 cm, which is higher than that of TATB (320 cm), but evidently lower than that of HMX (26 cm). This means that the characteristic drop height of TATB/HMX cocrystals increases 74 cm at least compared to that of raw

HMX, revealing that the impact sensitivity TATB/HMX cocrystals is evidently better than those of HMX.

3.8 Detonation Performance

The density and detonation performance of crystal explosive can be dramatically changed via cocrystallization [23]. The parameters of samples including TATB, HMX, and TATB/HMX cocrystal were predicted by EXPLO5 program [24] to evaluate the energetic properties and are listed in Table 5. The detonation velocity and pressure of TATB/HMX cocrystal are 9064.07 m/s and 36.96 GPa, respectively, and they are lower than those of HMX (9234.74 m/s, 38.86 GPa) but are more powerful than TATB (8624.92 m/s, 31.72 GPa). The properties of cocrystals met the requirements of high-energy insensitive explosives.

Table 5. Detonation performance of samples.

samples	Detonation performance			
	Density/ g/cm^3	Velocity/ m/s	Pressure/ GPa	Temperature/ K
TATB	1.940	8624.92	31.72	2944.6
HMX	1.905	9234.74	38.86	3687.7
TATB/HMX	1.915	9064.07	36.96	3469.7

4 Conclusion

TATB/HMX cocrystals were successfully obtained in a combination solvent [Emim]Ac/DMSO in a molar ratio of 5:95 at 80 °C by recrystallization. High temperature allowed the formation of superfine cocrystals. The TATB/HMX cocrystals agglomerated and were spherical in shape and range from 2 μm in size, as shown by the SEM data. The XRD pattern of cocrystals reveals the new crystal structure characteristics. The FT-Raman spectra indicate that the formation of cocrystals originates from the NO–H hydrogen bonding. The formation of cocrystals originates from the N–H…O hydrogen bonding between -NO_2 (HMX) and -NH_2 (TATB). Compared to raw HMX, the impact sensitivity of the cocrystals reduces obviously. The EXPLO5 program showed that the detonation performance of TATB/HMX can meet the requirements of modern high-energy insensitive explosives, and thus TATB/HMX is suitable for application in military and civilian fields.

References

[1] H. Bircher, Explosive substances and their applications: an overview, *CHIMIA International Journal for Chemistry* **2004**, *58*, 355–362.

[2] K. F. Grebenkin, Comparative Analysis of Physical Mechanisms of Detonation Initiation in HMX and in a low-Sensitive Explosive, *Combust. Explos. Shock Waves (Engl. Transl.)* **2009**, *45*, 78–87.

[3] J. P. Agrawal,Recent Trends in High-energy Materials, *Prog. Energy Combust. Sci.* **1998**, *24*,1–30.

[4] R. L. Simpson, P. A. Urtiew, D. L. Ornellas, G. L. Moody, K. J. Scribner, D. M. Hoffman,CL-20 Performance Exceeds That of HMX and its Sensitivity is Moderate, *Propellants Explos. Pyrotech.* **1997**, 249–255.

[5] N. Shan, M. J. Zaworotko, The Role of Cocrystals in Pharmaceutical, *Drug Discovery Today* **2008**, *13*, 440.

[6] F. Lara-Ochoa, G. Espinosa-Perez, Cocrystals Definitions, *Supramol. Chem.* **2007**, *19*, 553–557.

[7] C. B. Aakeröy, D. J. Salmon, Building Co-crystals with Molecular Sense and Supramolecular Sensibility, *CrystEngComm* **2005**, *7*, 439–448.

[8] A K Sikder, N Sikder, A Review of Advanced High Performance, Insensitive and Thermally Stable Energetic Materials Emerging for Military and Space Applications, *J. Hazard. Mater.* **2004**, *112*, 1–15.

[9] O. Bolton, L. R. Simke, P. F. Pagoria, A. J. Matzger, High Power Explosive with Good Sensitivity, A 2:1 Cocrystal of CL-20:HMX, *Cryst. Growth Des.* **2012**, *12*, 4311.

[10] C. W. An, H. Q. Li, B. Y. Ye, J. Y. Wang, Nano-CL-20/HMX Cocrystal Explosive for Significantly Reduced Mechanical Sensitivity, *J. Nanomater.* **2017**, *5*, 7.

[11] H. Lin, S. G. Zhu, H. Z. Li, X. H. Peng, Synthesis, Characterization, AIM and NBO Analysis of HMX/DMI Cocrystal Explosive, *J. Mol. Struct.* **2013**, *1048*, 339–348.

[12] H. Lin, S. G. Zhu, L. Zhang, X. H. Peng, H. Z. LI, Synthesis and First Principles Investigation of HMX/NMP Cocrystal Explosive, *J. Energ. Mater.* **2013**, *31*, 261–272.

[13] H. Lin, J. F. Chen, S. G. Zhu, H. Z. Li, Y. Huang, Synthesis, Characterization, Detonation Performance, and DFT Calculation of HMX/PNO Cocrystal Explosive, *J. Energ. Mater.* **2016**, *35*, 95–108.

[14] H. Lin, S. G. Zhu, L. Zhang, X. H. Peng, P. Y. Chen, H. Z. Li, Intermolecular Interactions, Thermodynamic Properties, Crystal Structure, and Detonation Performance of HMX/NTO Cocrystal Explosive, *Int. J. Quantum Chem.* **2013**, *113*, 1591–1599.

[15] H. Lin, S. G. Zhu, H. Z Li, X. H. Peng, Structure and Detonation Performance of a Novel HMX/LLM-105 Cocrystal Explosive, *J. Phys. Org. Chem.* **2013**, *26*, 898–907.

[16] H. Q. Li, C. G. An, W. J. Guo, X. H. Geng, J. Y. Wang, W. Z. Xu, Preparation and Performance of Nano HMX/TNT Cocrystals, *Propellants Explos. Pyrotech.* **2015**, *40*, 652–658.

[17] V. M. Boddu, D. S. Viswanath, T. K. Ghosh, R. Damavarapu, 2,4,6-Triamino-1,3,5-Trinitrobenzene (TATB) and TATB-based Formulations-a Review, *J. Hazard. Mater.* **2010**, *181*, 1–8.

[18] C. Y. Wei, H. Huang, X. H. Duan, C. H. Pei, Structures and Properties Prediction of HMX/TATB Co-Crystal, *Propellants Explos. Pyrotech.* **2011**, *36*, 416–423.

[19] National Military Standard of China, Experimental Methods of Sensitivity and Safety GJB/772A-97, **1997** (in Chinese).

[20] J. Y. Wang, B. Y. Ye, C. W. An, B. D. Wu, H. Q. Li, Y. J. Wei, Preparation and Properties of Surface-Coated HMX with Viton and Graphene Oxide, *J. Energ. Mater.* **2016**, *34*, 235–245.

[21] H. G. Brittain, Vibrational Spectroscopic Studies of Cocrystals and Salts. 4. Cocrystal Products Formed by Benzylamine, α-Methylbenzylamine, and Their Chloride Salts, *Cryst. Growth Des.* **2011**, *11*, 2500–2509.

[22] M. A. Elbagerma, H. G. M. Edwards, T. Munshi, M. D. Hargreaves, P. Matousek, I. J. Scowen, Characterization of New Cocrystals by Raman Spectroscopy, Powder X-ray Diffraction, Differential

Scanning Calorimetry, and Transmission Raman Spectroscopy, *Cryst. Growth Des.* **2010**, *10*, 2360–2371.

[23] O. Bolton, A. J. Matzger, Improved Stability and Smart-Material Functionality Realized in an Energetic Cocrystal, *Angew. Chem. Int. Ed.* **2011**, *50*, 8960–8963; *Angew. Chem.* **2011**, *123*, 9122–9125.

[24] M. Suceska, Evaluation of Detonation Energy from EXPLO5 Computer Code Result, *Propellants Explos. Pyrotech.* **1999**, *24*, 280–285.

Received: January 4, 2018
Revised: June 21, 2018
Published online: July 22, 2018

